E-Journal of Advanced Maintenance Vol.4 No.1 (2012) 5-25
Japan Society of Maintenology

Capability of Ultrasonic Testing for Cast Austenitic Stainless Steel in Japanese Pressurized Water Reactors

Kazunobu SAKAMOTO[1,*], Takashi FURUKAWA[2], Ichiro KOMURA[2], Youitsu YAGIHASHI[2] and Tsuyoshi MIHARA[3]

[1] *Japan Nuclear Energy Safety Organization, 4-1-28, Toranomon, Minato-ku, Tokyo, 105-0001, Japan*
[2] *Japan Power Engineering and Inspection Corporation, 14-1, Benten-cho, Tsurumi-ku, Yokohama, 230-0044, Japan*
[3]*University of Toyama, 3190 Gofuku, Toyama-shi, Toyama, 930-8555, Japan.*

ABSTRACT

Flaw detection and sizing capabilities for cast austenitic stainless steel (CASS) which is widely used in primary loop of Japanese pressurized water reactors (PWR) are studied using conventional UT techniques currently applied on the CASS in in-service inspection program in Japan, Phased Array (PA) technique, as well as inspection by large size probe. The objective of the study was to make sure the accuracy of detection and sizing of inner surface flaws from the outside diameter piping surface by ultrasonic testing (UT) of which primary mode is longitudinal wave.

The result showed that currently available UT techniques are capable to detect the small cracks stable enough under postulated accident loads even after the thermal aging. With regard to the sizing capability, the result suggested that some consideration shall be taken into account when applying the technique if cracks were detected and technical breakthrough might be expected in the future.

KEYWORDS

Cast austenitic stainless steel, CASS, Pressurized Water Reactor, PWR, Ultrasonic testing, UT

ARTICLE INFORMATION

Article history:
Received 26, Dec 2011
Accepted 22, May 2012

1. Introduction

Cast austenitic stainless steel (CASS) is widely used in reactor coolant piping systems in Japanese pressurized water reactors (PWRs) due to its corrosion resistance, high weldability and relatively low cost. To maintain the integrity of the piping systems, the Rules on the Fitness-for-Service for Nuclear Power Plants of Japan Society of Mechanical Engineers (JSME) Code requires periodic ultrasonic inspection on welds in the reactor coolant piping as an in-service inspection program [1]. However it is well known that coarse grained and anisotropic crystal structure makes it difficult to detect and size flaws in the cast stainless steel components by ultrasonic technique due to beam skewing, dispersion and unexpected attenuation. Hence the miss or false calling of the flaws and the deterioration of sizing performance are of great concerns in the ultrasonic testing (UT) for CASS piping not only in Japan but also other countries which have PWRs, because the systems are safety related.

Under such circumstances, a variety of researches, such as UT technique and probe development, signal processing, study on the grain structures, have been carried out to cope with this problem [2-6]. With regard to the UT probes, large size probe which generates high energy ultrasound and using low frequency probe etc. have been proposed [7]. In Europe, round robin test were performed using CASS weld mockup under the Program for the Inspection of Steel Components (PISC) sponsored by European Communities [8, 9].

In Japan, national research program entitled “Development on Standards and Guides for Formation of Up graded Inspection System on NPP” have also studied the UT capability for CASS with the limited test pieces and available UT technique about a decade ago. At that time, the project

Corresponding author, E-mail: sakamoto-kazunobu@jnes.go.jp

had concluded that flaw was recognized when the depth is greater than 20% of wall thickness, but impossible to verify the sizing capability of flaw length and depth [10]. Over the last decade, UT techniques for CASS have been advanced including low frequency phased array methodology and application of large sized twin crystal transducer. However, to date, no answer to the question about the flaw detection and sizing capability of the UT for CASS is available.

The objective of this paper is to comprehend the UT capability for flaws in CASS piping and to make sure the adequacy of current in-service inspection requirement. For this purpose, welded joint specimens, whose material, size, dimension and welding method are identical to the actual PWR plant, are prepared.

2. Materials

CASS specimens and large piping segment with inside surface (ID) connected fatigue crack are prepared as summarized in Table 1. Since the destructive test was not carried out, the flaw depths of JTP A, JTP B and Mockup B used as actual size are based on the manufacturing record. The information of ferrite contents other than JTP B is not described because the tendency of wave propagation is not affected by the ferrite contents itself but is heavily rely on the grain structures [11].

Table 1. Summary of the materials applied in the study

Specimen	Specification
JTP A	Type: Centrifugally CASS (CCASS) piping to Statically CASS (SCASS) piping butt weld Material: SA351 CF-8M Size: 200mm(Width: W)×500mm(Length: L)×77.8mm(Thickness: t) Flaw: Circumferential fatigue crack at ID surface along with weld line, induced by three point bend cyclic loading Number of specimen: 4
JTP B	Type: CCASS piping Material: CF-8M (CCASS) Size: 200W×200L×70t Flaw: Circumferential fatigue crack, induced by cyclic loading Number of specimen: 4
KPS-04	Type: Safe-end (Forging) to CCASS piping butt weld Material: Safe end (Upper stream: U/S):SA430 Gr.316L Piping (Down Stream: D/S): SA351 Gr.CF8A Size: ϕ 736.6mm (ID, 120degree)×632mmL×U/S 74.6mmt, D/S 62mmt Flaw: 3 circumferential and 2 axial thermal fatigue cracks at ID surface along with weld line Number of specimen: 1
KPS-05	Type: CCASS piping to CCASS piping butt weld Material: SA351 Gr.CF8A Size: ϕ 736.6mm (ID, 60degree)×629mmL×62mmt Flaw: 2 circumferential and 1 axial thermal fatigue cracks at ID surface along with weld line Number of specimen: 1
Mockup A	Type: CCASS piping to SCASS elbow butt weld Material: SA351 CF-8M (CCASS) Size: Piping: ϕ 836mm(OD)×500mmL×69mmt Elbow: ϕ 900.1mm(OD)×110mmt～111.6mmt Flaw: 2 circumferential fatigue cracks at ID surface along with weld line, induced by cyclic loading Number of specimen: 1
Mockup B	Type: CCASS piping to SCASS elbow butt weld Material: SA351 CF-8M (CCASS) Size: Piping: ϕ 837.7mm(OD)×500mmL×70mmt Elbow: ϕ 900.1mm(OD)×90mmt～110mmt Flaw: A circumferential fatigue crack at ID surface along with weld line, induced by cyclic loading Number of specimen: 1

The series of JTP A are the specimens of centrifugally CASS (CCASS) to Statically CASS (SCASS) butt weld by Gas Tungsten Arc Welding (GTAW), whose material, dimension and welding method are identical to the most recent CASS main coolant piping in Japanese PWRs. Fig. 1 shows the profile and flaw specification of the JTP A series specimens. Circumferential fatigue cracks are induced along with the welding line by three point bend cyclic loading. To create the fatigue crack, excess metal was welded on the ID surface and induced EDM notch as a starter of fatigue crack at first. After the fatigue crack propagation the starter notch and excess metal was removed. Once the round 1 measurement finished, fatigue cracks were propagated to be applied to the round 2 measurement to make use of limited specimens.

JTP B-1 through B-4 are the specimens of centrifugally CASS (CCASS) with circumferential fatigue cracks simulating main coolant piping of Japanese PWRs. Fig. 2 shows the profile and flaw specification of the JTP B series specimens. A circumferential fatigue crack was induced at the center of each specimen by cyclic mechanical load.

KPS-04 is the specimen of forged stainless steel safe-end to SCASS butt weld. KPS-05 is the specimen of CCASS to CCASS butt weld. KPS-04 and KPS-05, representing the main coolant piping system of Westinghouse PWRs in Korea, have circumferential and axial thermal fatigue cracks manufactured by Sonaspection International Ltd. Fig. 3 and Fig. 4 show the profile and flaw specification of the KPS-04 and KPS-05 respectively.

Mockup A is the piping segment of CCASS piping to SCASS elbow butt weld by GTAW and Shielded Metal Arc Welding (SMAW) plus Submerged Arc Welding (SAW) simulating Japanese main coolant piping system as shown in Fig. 5. Fatigue cracks are induced at both sides of the weld by cyclic mechanical load. Flaw depth described in Fig. 5 is the measurement value by UT from the ID surface carried out as a finger printing.

Mockup B is the piping segment of CCASS piping to SCASS elbow butt weld by GTAW plus SAW, also simulating Japanese main coolant piping system as shown in Fig. 6. A fatigue crack at the elbow along with the welding line is induced by cyclic mechanical load.

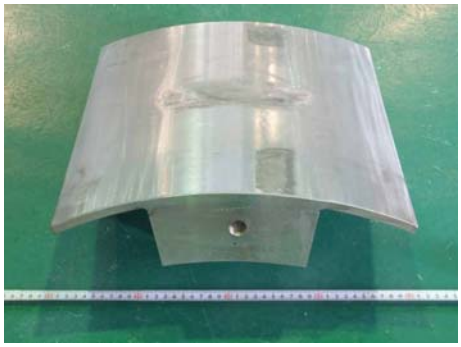

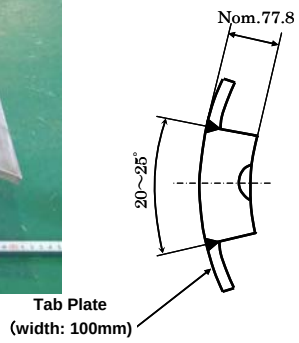

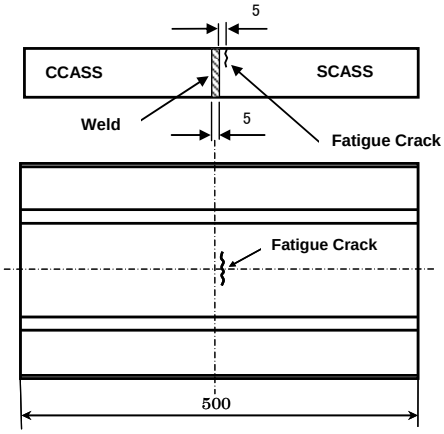

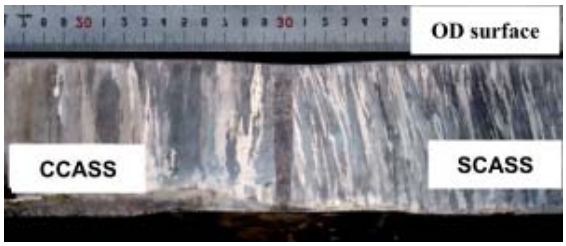

Macrograph of the cross section

Specification of flaw

Specimen	Flaw location	Flaw size (mm)	
		Depth	Length
JTP A-1	SCASS	3.8	36
		11.8	50
JTP A-2	SCASS	8.6	62
		17.4	66
JTP A-3	CCASS	4.3	36
		12.4	42
JTP A-4	CCASS	8.4	38
		15.8	58

Fig. 1. JTP A series specimens

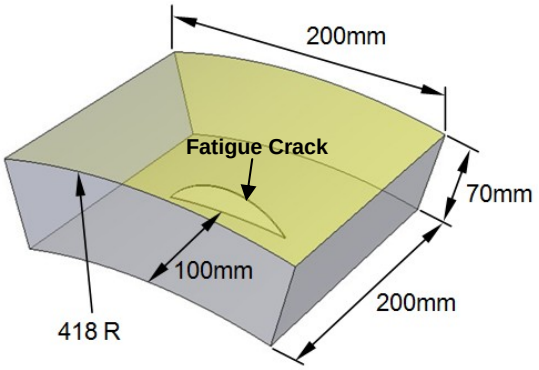

Specification of flaw

Specimen	Ferrite contents	Flaw Size (mm)	
		Depth	Length
JTP B-1	15%	7	46.8
JTP B-2	15%	14	56.4
JTP B-3	15%	21	76.0
JTP B-4	8%	35	108.0

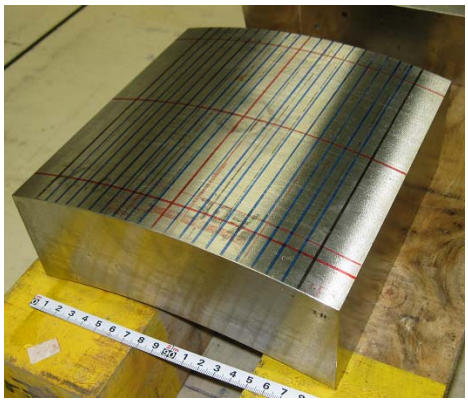

Fig. 2. JTP B series specimens

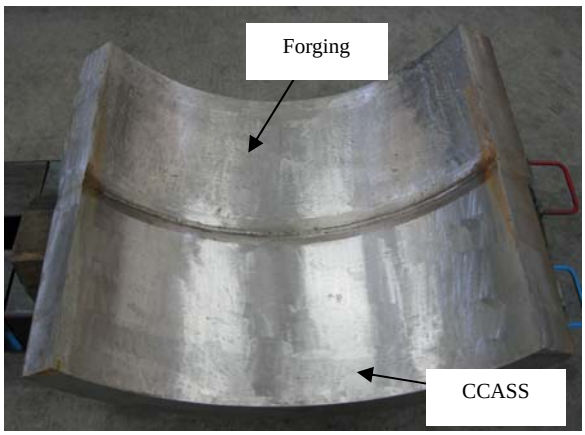

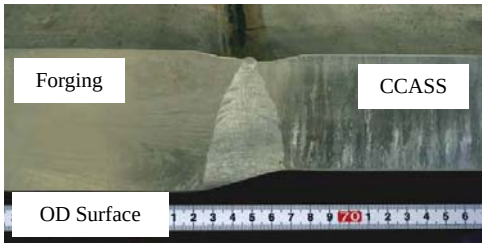

Macrograph of the cross section

Specification of flaw

Flaw #	Flaw direction	Flaw size (mm)	
		Depth	Length
No1	Circumferential	56.2	151.6
No2	Axial	15.9	51.0
No3	Axial	12.5	27.8
No4	Circumferential	30.8	71.5
No5	Circumferential	19.7	101.0

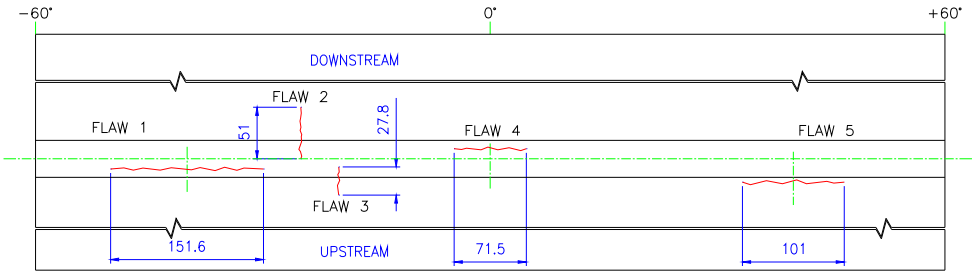

Flaw location

Fig. 3. KPS-04 Specimen

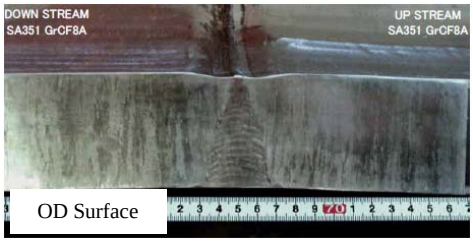

Macrograph of the cross section

Specification of flaw

Flaw #	Flaw direction	Flaw size (mm)	
		Depth	Length
No1	Circumferential	46.1	128.5
No2	Axial	14	41
No3	Circumferential	10.9	96.5

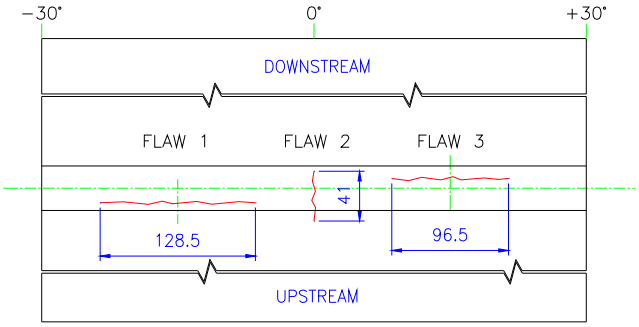

Flaw location

Fig. 4. KPS-05 Specimen

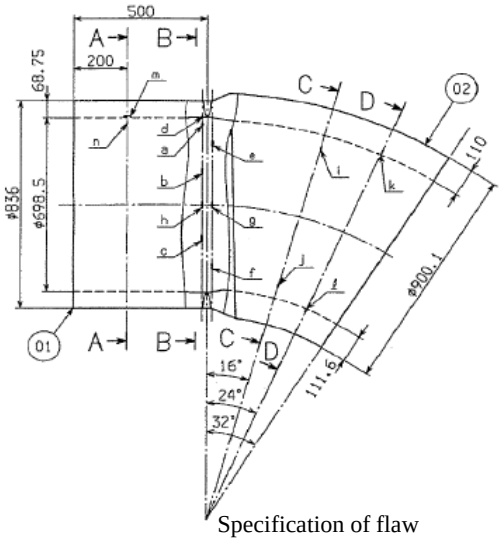

Specification of flaw

Flaw #	Flaw type	Flaw size (mm)		Flaw location
		Depth	Length	
Ag	Fatigue (circumferential)	19	43	Elbow (base metal), along with weld line
Ah	Fatigue (circumferential)	12	74	Piping (base metal), along with weld line

Fig. 5. Mockup A Specimen

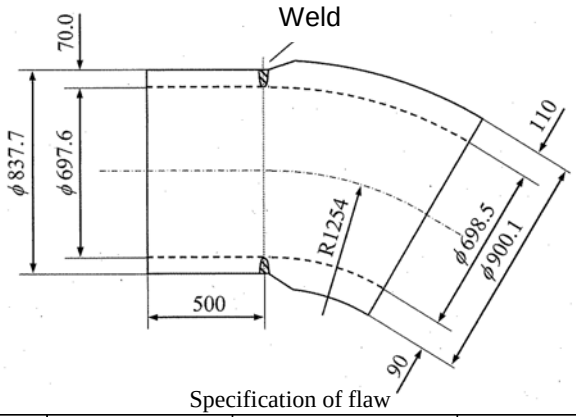

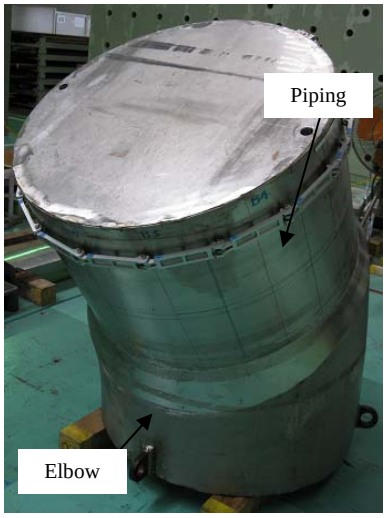

Specification of flaw

Flaw #	Flaw type	Flaw size (mm)		Flaw location
		Depth	Length	
B1	Fatigue (circumferential)	20.0	68.8	Elbow (base metal), along with weld line

Fig. 6. Mockup B Specimen

3. Applied UT techniques

The objective of examination is to make sure the accuracy of detection and sizing of ID cracks from the outside diameter (OD) piping surface by UT of which primary mode is longitudinal wave. Flaw detection and sizing were performed by two teams, Team I and Team II, using conventional UT techniques currently applied on the CASS in in-service inspection program in Japan, matrix Phased Array Ultrasonic Testing (PAUT) technique, as well as large size probe. Team I applied conventional UT and PA technique as shown in Table 2. Team II focused on the inspection using large size probe, of which type was twin crystals with angled longitudinal waves from the spherical shape of oscillator as presented in Table 3 [8].

Inspection personnel of Team I performed this test have certifications of UT Level 2 or 3 of Japanese Industrial Standard (JIS) Z2305 [12] or Japanese Nondestructive Inspection Standard (NDIS) 0601 [13]. The Team II data were obtained by the inspection personnel who have sufficient experience and capability equivalent to UT Level 2 or 3 although no certification obtained.

Table 2. Applied UT probe by Team I (Conventional UT, PAUT)

Probe	PAUT		Conventional		
	128ch Matrix PAUT	128ch Matrix PAUT	1C40x30 LAD45A	1C30x20 LAD36	1C38, 1LA36 (V392)
Frequency	0.5MHz	1MHz	1MHz	1MHz	1MHz
Mode	L	L	L	L	L
Incident angle	～55°	～55°	45°	36°	36°

Table 3. Applied UT probe by Team II (Large size probe)

Probe	A	B	C	D	E	F
Probe dimensions (mm)	100x100x80	100x100x80	100x100x80	100x100x80	100x100x80	100x100x80
Frequency	1MHz	1MHz	1MHz	1MHz	1MHz	1MHz
Mode	L	L	L	L	L	L
Shape of oscillator	spherical	spherical	spherical	spherical	spherical	spherical
Incident angle	40.7°	40.7°	45.0°	47.4°	49.0°	51.0°
Focusing depth (mm)	65-75	65-75	45-65	40-60	40-65	40-65

4. Experiments and discussion

4.1. Flaw detection capability

Table 4 summarizes the result of flaw detectability. All flaws from 3.8mm to 56.2mm in depth was detected by Matrix PAUT and Large size Probes. Conventional UT could detect more than 90% of flaws.

Table 4. Summary of the flaw detection capability

Specimen	Flaw Specification						Matrix PAUT		Conventional UT			UT by Large size probe					
	Flaw #	Type	Direction**	Location	Depth (mm)	Length (mm)	0.5MHz	1MHz	1C40×30 LAD45	1C30×20 LAD36	V392	A	B	C	D	E	F
JTP A-1	-	Fatigue	C	SCASS	3.8	36	○	○	×	○	○	○	○	○	○	*1	*1
	-	Fatigue	C	SCASS	11.8	50	○	○	○	○	○	○	○	○	○	○	○
JTP A-2	-	Fatigue	C	SCASS	8.6	62	○	○	○*3	○	○	○	○	○	○	*1	*1
	-	Fatigue	C	SCASS	17.4	66	○	○	○	○	○	○	○	○	○	○	○
JTP A-3	-	Fatigue	C	CCASS	4.3	36	○	○	○*3	○*3	○*3	○	○	○	○	*1	*1
	-	Fatigue	C	CCASS	12.4	42	○	○	○	○	○	○	○	○	○	○	○
JTP A-4	-	Fatigue	C	CCASS	8.4	38	○	○	○*3	○*3	○	○	○	○	○	*1	*1
	-	Fatigue	C	CCASS	15.8	58	○	○	○	○	○	○	○	○	○	○	○
JTP B-1	-	Fatigue	C	CCASS	7	46.8	○	○	○	○	○	○	○	○	○	○	○
JTP B-2	-	Fatigue	C	CCASS	14	56.4	○	○	○	○	○	○	○	○	○	○	○
JTP B-3	-	Fatigue	C	CCASS	21	76	○	○	○	○	○	○	○	○	○	○	○
JTP B-4	-	Fatigue	C	CCASS	35	108	○	○	○	○	○	○	○	○	○	○	○
KPS-04	No1	Fatigue	C	Forging	56.2	151.6	○	○	○	○	○	○*2	○*2	○	○	○	○
	No2	Fatigue	A	CCASS	15.9	51	○	○	*1	*1	○	*1	*1	*1	*1	*1	*1
	No3	Fatigue	A	Forging	12.5	27.8	○	○	*1	○	○	*1	*1	*1	*1	*1	*1
	No4	Fatigue	C	CCASS	30.8	71.5	○	○	○	○*2	○*2	○	○	○	○	○	○
	No5	Fatigue	C	Forging	19.7	101	○	○*3	○	○*2	○*2	○*2	○*2	○*2	○*2	○*2	○*2
KPS-05	No1	Fatigue	C	CCASS	46.1	128.5	○	○	○	○	○	○	○	○	○	○	○
	No2	Fatigue	A	CCASS	14	41	○	○	△*3	○	○	*1	*1	*1	*1	*1	*1
	No3	Fatigue	C	CCASS	10.9	96.5	○	○	○	○	○	○	○	○	○	○	○
Mockup A	Ag	Fatigue	C	SCASS	19	43	○*2	○*2	×*2	○*2	○*2	○*2	○*2	○*2	○*2	○*2	○*2
	Ah	Fatigue	C	CCASS	12	74	○*2	○*2	○*2	○*2	○*2	○*2	○*2	○*2	○*2	○*2	○*2
Mockup B	B1	Fatigue	C	SCASS	20.0	68.8	○*2	○*2	○*2	×*2	×*2	○*2	○*2	○*2	○*2	○*2	○*2

○: Clearly Detected (SN＞2), △: Detected (SN≦2), ×: Undetected
**: C: Circumferential, A: Axial
*1: Inspection was not carried out
*2:The inspection was carried out only from one side (due to the restriction of probe accessibility, etc.)
*3: Able to detect from one side (not detected from the other side)

Fig. 7 shows the relationship between flaw depth and detectability together with the Probability of Detection (POD) curve obtained by logistic regression model. Although a various POD curves were proposed, a logistic regression model proposed by Pacific Northwest National Lab was applied in this study to relate POD to flaw size described as follows [14];

$$POD(a) = \frac{1}{1+\exp\left(-\beta_1 - \beta_2 a\right)} \qquad \text{----------} \quad (1)$$

α : flaw size
β_1, β_2: Unknown parameters to be determined by the regression algorithm
note: Estimates produced by the algorithm are maximum-likelihood estimates.
The regression fits included data for flaw size zero.

The minimum value of POD at the 3.8 mm of flaw depth was 0.976. The conservatism of the structure integrity for the CASS piping system postulating 60 years thermal aging with flaws of 20% wall thickness in depth and 100% wall thickness in length was verified by the research program by Japan Nuclear Energy Safety Organization [15]. Based on this knowledge, it can be said that currently available UT techniques are capable to detect the small cracks stable enough under postulated accident loads even after the thermal aging referring the POD analysis. However it should be noted that around 20mm depth fatigue cracks were not detected by some of conventional UT techniques. Considering this fact, continuous effort such as selecting the appropriate probe (e.g. PAUT probe) and training of the inspection personnel is essential, as well as the technical development to improve the flaw detection capability.

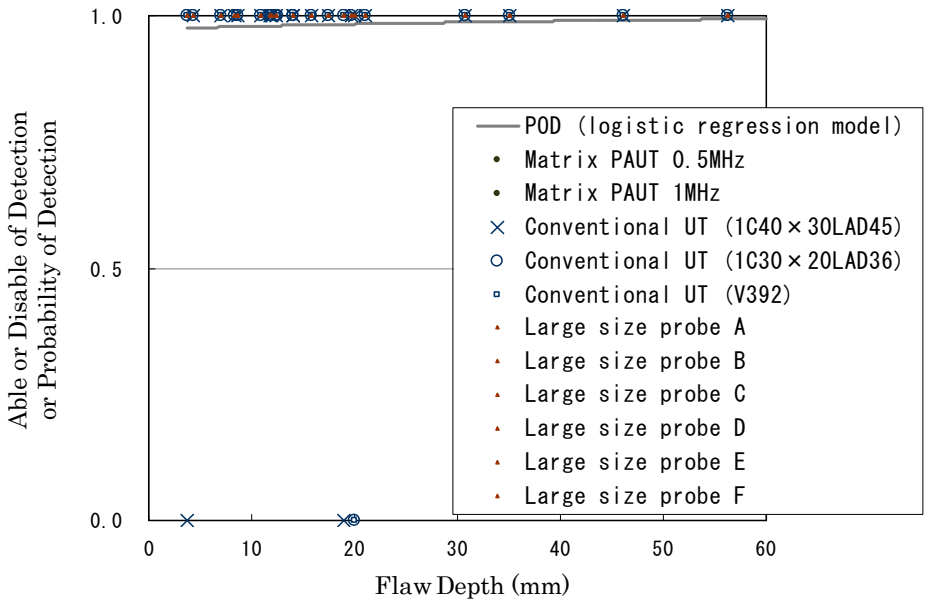

Fig. 7. Flaw depth vs. detectability

4.2. Flaw depth sizing capability

Table 5 summarizes the result of flaw depth sizing test. Here, the deeper call of the measurement results was described in the table when the measurement was carried out from both side of the flaw. As presented in the table, the depth sizing itself was unable for shallow flaw by currently available UT techniques due to the difficulty of identifying tip echo.

Fig. 8 illustrates the relationship between flaw depth and the able / disable points plotted from the examination for each flaw by all measurement methods, conventional UT, matrix PAUT and measurement by large size probe respectively. Logistic regression analysis result using the model of equation (1) which means probability of depth measurement is also presented in the figures. The result implies that it is almost impossible to size the depth of early stage flaws such as less than 20% of wall thickness in the main coolant piping systems with currently available UT techniques. When a flaw depth exceeded 20mm, possibility of depth measurement became asymptotic to 1.

Fig. 9 shows the relationship between actual flaw depth and measurement result using data that was able to size. The root mean square error (RMSE) of the flaw depth sizing by all measurement techniques applied in this study was 4.1 mm.

The RMSE by each measurement method was 5.6 mm for conventional UT, 4.5 mm for matrix PAUT, and 3.2 mm for measurement by large size probe, respectively. Measurement by large size probe showed the best result in every aspect as described in the figure among the three methods. Focusing on the measurement by large size probe, Probes C and D show the better sizing accuracy than other probes. Matrix PAUT was able to size the depth with good accuracy for deeper flaws more

than 30 mm. Although the depth sizing itself was impossible for shallow flaw, the sizing accuracy was relatively good when the tip echo was identified. On the other hand, it can be said that currently used conventional UT is not adequate to size the flaw depth.

Referring the Performance Demonstration (PD) examination of inter granular stress corrosion cracking (IGSCC) depth sizing in Japan although the flaw type was different, the criteria of RMSE with below 3.2 mm and not allowing the any underestimation exceeding 4.4 mm was not satisfied yet by any measurement method [16].

Current JSME Code does not require any specific description of the UT for CASS. However, the results suggested that special consideration shall be taken into account to carry out the depth sizing for CASS piping.

Table 5. Summary of the flaw depth sizing test result

Specimen	Flaw Specification					Matrix PAUT		Conventional UT			UT by Large size probe					
	Flaw #	Direction**	Location	Depth (mm)	Length (mm)	0.5MHz	1MHz	1C40×30 LAD45	1C30×20 LAD36	V392	A	B	C	D	E	F
JTP A-1	-	C	SCASS	3.8	36	×	×	✗	×	×	×	×	×	×	*1	*1
	-	C	SCASS	11.8	50	9.8*4	17.5	×	×	×	13.5	11.6*4	11.3*4	10.7*4	11.1*4	9.3*4
JTP A-2	-	C	SCASS	8.6	62	18.1*4	15.5	×*3	×	×	7.8*4	9.4*4	×	×	*1	*1
	-	C	SCASS	17.4	66	20.5	24.4	16.1	19.7*4	24.4*4	14.6	×	13.8*4	11.7	11.6*4	×
JTP A-3	-	C	CCASS	4.3	36	×	×	×*3	×*3	×*3	×	×	×	×	*1	*1
	-	C	CCASS	12.4	42	17.1	18.7*4	11.7*4	×	×	×	×	11.3*4	12.6	12.9	9.9
JTP A-4	-	C	CCASS	8.4	38	×	×	×*3	×*3	×	13.5*4	×	×	×	*1	*1
	-	C	CCASS	15.8	58	17.6	19.9	20.7	×	14.8*4	15.5*4	×	12.5*4	20.7	19.6	16.7*4
JTP B-1	-	C	CCASS	7	46.8	×	×	×	6.6*4	×	×	8.0*4	6.7*4	5.2*4	10.0*4	×
JTP B-2	-	C	CCASS	14	56.4	13.6*4	12.4	×	×	×	15.6	16.0	12.1	14.6	12.9	12.1
JTP B-3	-	C	CCASS	21	76	20.8	24.9	×	24.9*4	×	22.6	20.8	19.9	19.7	18.5	22.8
JTP B-4	-	C	CCASS	35	108	35.0	39.1	35.9*4	×	38.6	36.4	38.4	36.5	33.9	36.3	34.1
KPS-04	No1	C	Forging	56.2	151.6	58.4*5	59.1*5	54.0*5	48.7*5	51.4*5	55.7*2	56.7*2	53.7*5	55.3*5	52.2*5	52.0*5
	No2	A	CCASS	15.9	51	13.4*4	19.7*4	*1	*1	13.0	*1	*1	*1	*1	*1	*1
	No3	A	Forging	12.5	27.8	×	6.2*4	*1	×	3.5*4	*1	*1	*1	*1	*1	*1
	No4	C	CCASS	30.8	71.5	33.6	32.4	26.3	24.2*2	29.1*2	16.2*5	20*5	26.4*5	30.3*5	26.2*5	35.3*5
	No5	C	Forging	19.7	101	25.2*5	17.0*3	16.4*5	17.8*2	16.4*2	19.2*2	20.6*2	18.6*2	17.3*2	17.3*2	15.6*2
KPS-05	No1	C	CCASS	46.1	128.5	46.5	45.3	45.6	25.7*4	38.0	45.5*4	46.9*4	44.3	45.7	45.1	44.4
	No2	A	CCASS	14	41	13.5	12.3	×*3	13.6*4	12.0	*1	*1	*1	*1	*1	*1
	No3	C	CCASS	10.9	96.5	16.0	16.0	11.0	4.3*4	×	11.0*4	10.7*4	10.8	11.1	10.0	10.0
Mockup A	Ag	C	SCASS	19	43	×*2	×*2	✗*2	×*2	×*2	×*2	×*2	×*2	×*2	×*2	×*2
	Ah	C	CCASS	12	74	×*2	×*2	15.0*2	×*2	×*2	×*2	11.9*2	12.5*2	10.8*2	14.1*2	11.3*2
Mockup B	B1	C	SCASS	20.0	68.8	31.8*2	18.2*2	14.7*2	✗*2	✗*2	11.5*2	14.1*2	18.6*2	18.4*2	×*2	22.1*2

(mm)

×: Unable to size, ✗: Flaw was not detected
**: C: Circumferential, A: Axial
*1: Inspection was not carried out
*2: The inspection was carried out only from one side (due to the restriction of probe accessibility, etc.)
*3: Able to detect from one side (not detected from the other side)
*4: Able to size from one side (not able to size from the other side)
*5: Sizing was carried out only from CCASS side although flaw was detected by the inspection from both sides

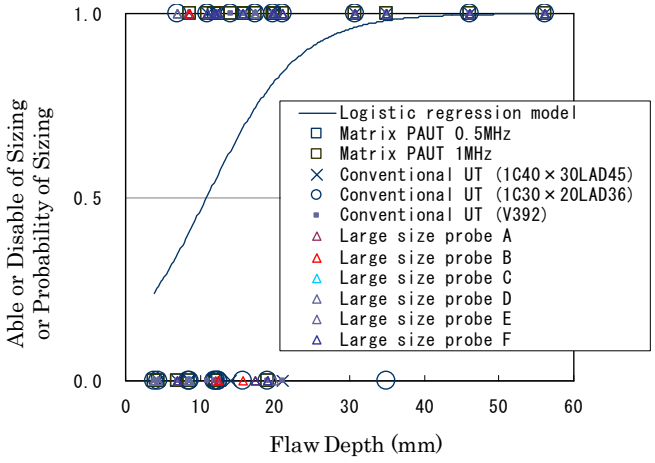

(1) All measurement methods

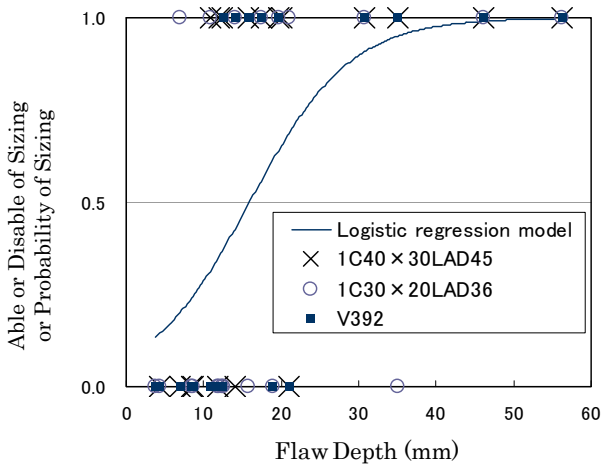

(2) Conventional UT

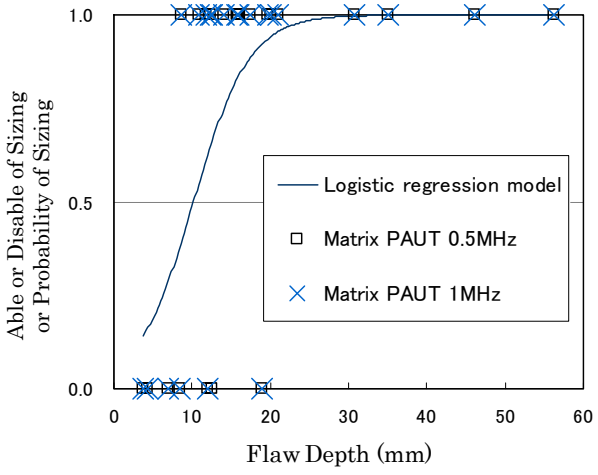

(3) Matrix PAUT

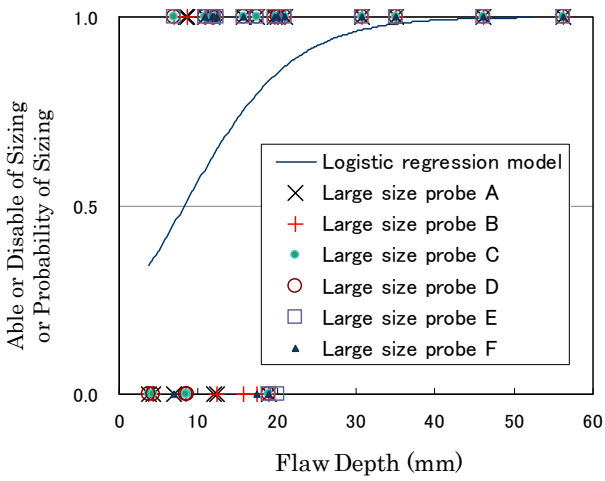

(4) UT by Large size probe

Fig. 8. Probability of depth measurement

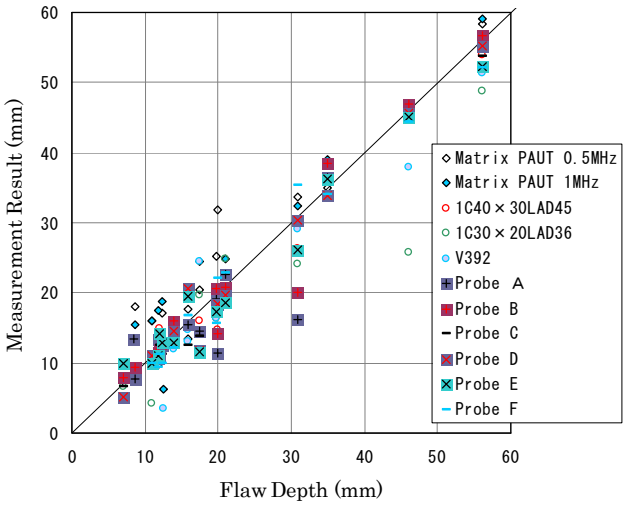

Max. error of overestimation: 11.8mm
Max. error of underestimation: -20.4mm
Ave. error: -0.5mm
Standard deviation of errors: 4.1mm
RMSE: 4.1mm

(1) All measurement methods

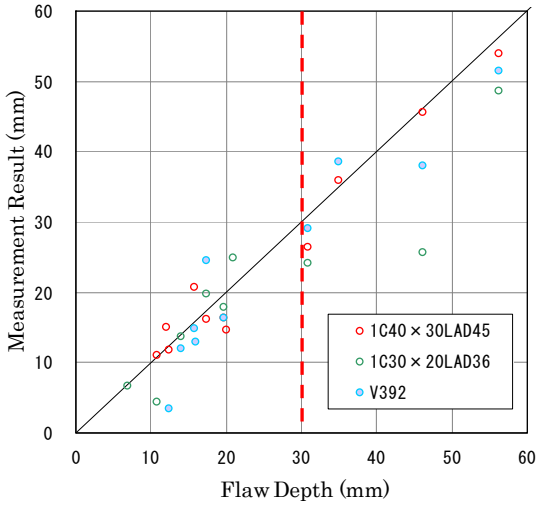

Max. error of overestimation: 7.0mm
Max. error of underestimation: -20.4mm
Ave. error: -2.3mm
Standard deviation of errors: 5.2mm
RMSE: 5.6mm

(2) Conventional UT

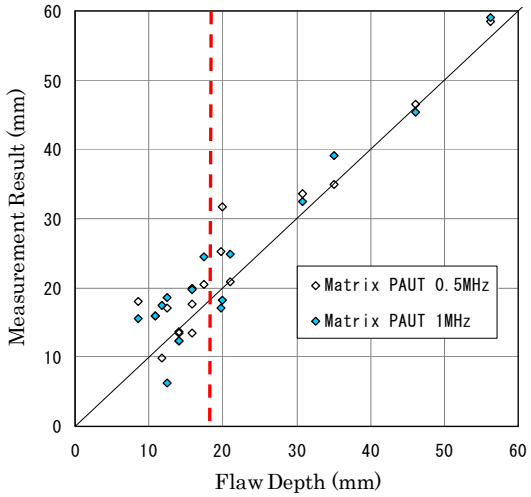

Max. error of overestimation: 11.8mm
Max. error of underestimation: -6.3mm
Ave. error: 2.4mm
Standard deviation of errors: .3.9mm
RMSE: 4.5mm

(3) Matrix PAUT

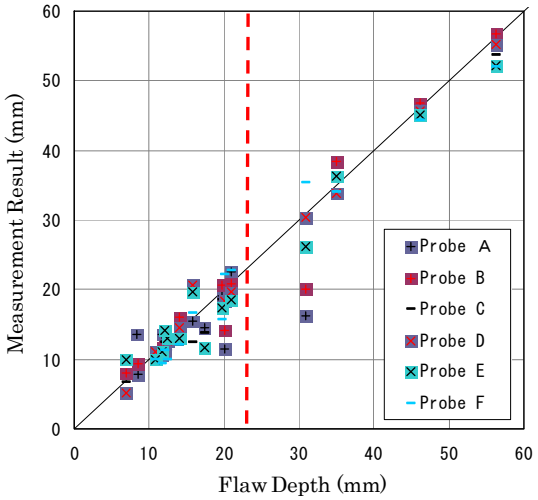

Max. error of overestimation: 5.1mm
Max. error of underestimation: -14.6mm
Ave. error: -1.0mm
Standard deviation of errors: 3.0mm
RMSE: 3.2mm

(4) UT by Large size probe

Fig. 9. Flaw depth sizing accuracy
Note: Red broken lines in the figure correspond to 90% of probability of sizing

4.3. Flaw length sizing capability

Flaw length was evaluated as loss of signal (S/N <1) for all measurement techniques. The result on flaw length sizing by each inspection methods is tabulated in Table 6. The bigger call of the

measurement results was described in the Table 6 when the measurement was carried out from both side of the flaw.

Fig. 10 illustrates the comparison between actual flaw length and measurement result by all applied UT techniques. The RMSE of length sizing by all measurement techniques was 16.8 mm.

The RMSE by each measurement method was 20.0mm for conventional UT, 22.8 mm for matrix PAUT, and 11.1 mm for measurement by large size probe, respectively. The standard deviation of the errors by each measurement techniques are, 19.9 mm for conventional UT, 20.8 mm for matrix PAUT, and 9.7 mm for measurement by large size probe. Measurement by large size probe showed the best result in every aspect as described in the figure among the three methods which was same result with the study on flaw depth sizing. The acceptance criterion of American Society of Mechanical Engineers (ASME) Code is less than 19.05mm for the RMSE in length sizing, although no such limitation exists in Japanese requirements [17]. When applying this criterion, only the measurement by large size probe satisfies the requirement. Same as the depth sizing measurement, test results suggested that special consideration, such as selecting large size probe, shall be taken into account to carry out the sizing for CASS piping in the field regarding the length sizing.

Table 6. Summary of the flaw length sizing test result

Specimen	Flaw Specification					Matrix PAUT		Conventional UT			UT by Large size probe					
	Flaw #	Direction**	Location	Depth (mm)	Length (mm)	0.5MHz	1MHz	1C40×30 LAD45	1C30×20 LAD36	V392	A	B	C	D	E	F
JTP A-1	-	C	SCASS	3.8	36	26.7	90.2	×	30.1	23.4	33.2	32.0	29.8	44.9	*1	*1
	-	C	SCASS	11.8	50	78.5	126.9	23.4	40.1	66.8	57.0	55.1	60.4	45.7	62.8	67.5
JTP A-2	-	C	SCASS	8.6	62	53.4	86.8	40.1*3	63.5	50.1	60.0	68.6	67.5	60.0	*1	*1
	-	C	SCASS	17.4	66	76.8	106.9	70.1	73.5	90.2	78.0	85.8	75.2	76.7	72.6	82.0
JTP A-3	-	C	CCASS	4.3	36	60.1	23.4	16.7*3	16.7*3	23.4*3	27.6	25.9	33.2	37.8	*1	*1
	-	C	CCASS	12.4	42	66.8	50.1	50.1	80.2	30.1	52.9	54.6	60.6	61.0	52.6	57.4
JTP A-4	-	C	CCASS	8.4	38	50.1	40.1	26.7*3	33.4*3	90.2	52.0	53.2	49.8	47.8	*1	*1
	-	C	CCASS	15.8	58	79.3	46.8	36.7	80.2	103.5	58.5	60.5	52.8	51.4	46.2	53.3
JTP B-1	-	C	CCASS	7	46.8	66.6	63.5	56.6	58.3	73.3	59.3	57.1	56.4	50.3	53.4	52.2
JTP B-2	-	C	CCASS	14	56.4	73.3	70.2	66.6	56.6	53.3	74.5	77.2	67.8	66.5	60.2	68.3
JTP B-3	-	C	CCASS	21	76	93.3	103.6	86.6	94.9	89.9	88.8	84.2	88.3	84.7	88.0	87.8
JTP B-4	-	C	CCASS	35	108	106.6	100.2	76.6	96.6	109.9	99.4	97.9	95.7	86.9	94.6	94.3
KPS-04	No1	C	Forging	56.2	151.6	157.4	146.1	123.2	142.8	142.8	148.3*2	159.9*2	150.5	145.7	153.7	159.9
	No2	A	CCASS	15.9	51	28.0	24.0	*1	*1	32.0	*1	*1	*1	*1	*1	*1
	No3	A	Forging	12.5	27.8	20.0	44.0	*1	16.0	40.0	*1	*1	*1	*1	*1	*1
	No4	C	CCASS	30.8	71.5	85.6	92.4	90.7	81.3*2	92.4*2	86.7	92.4	83.2	82.8	88.9	89.2
	No5	C	Forging	19.7	101	102.9	112.9*3	124.5	102.9*2	109.6*2	102.6*2	104.6*2	100.9*2	104.0*2	104.3*2	100.9*2
KPS-05	No1	C	CCASS	46.1	128.5	150.6	143.7	147.1	150.6	164.3	150.0	151.6	142.4	147.6	138.0	138.9
	No2	A	CCASS	14	41	48.0	52.0	24.0*3	52.0	44.0	*1	*1	*1	*1	*1	*1
	No3	C	CCASS	10.9	96.5	97.5	112.9	106.1	102.7	102.7	104.4	104.6	101.5	100.0	98.0	100.9
Mockup A	Ag	C	SCASS	19	43	26.7*2	16.7*2	×*2	10.0*2	46.8*2	40.0*2	45.1*2	49.2*2	37.9*2	37.2*2	38.6*2
	Ah	C	CCASS	12	74	50.1*2	63.5*2	60.1*2	50.1*2	43.4*2	72.1*2	70.2*2	60.0*2	72.4*2	57.6*2	69.3*2
Mockup B	B1	C	SCASS	20.0	68.8	93.3*2	106.6*2	106.6*2	×*2	×*2	90.6*2	82.1*2	90.0*2	73.8*2	86.9*2	80.7*2

(mm)

×: Flaw was not detected (unable to size)
**: C: Circumferential, A: Axial
*1: Inspection was not carried out
*2:The inspection was carried out only from one side (due to the restriction of probe accessibility, etc.)
*3: Able to detect from one side (not detected from the other side)
*4: Able to size from one side (not able to size from the other side)
*5: Sizing was carried out only from CCASS side although flaw was detected by the inspection from both sides

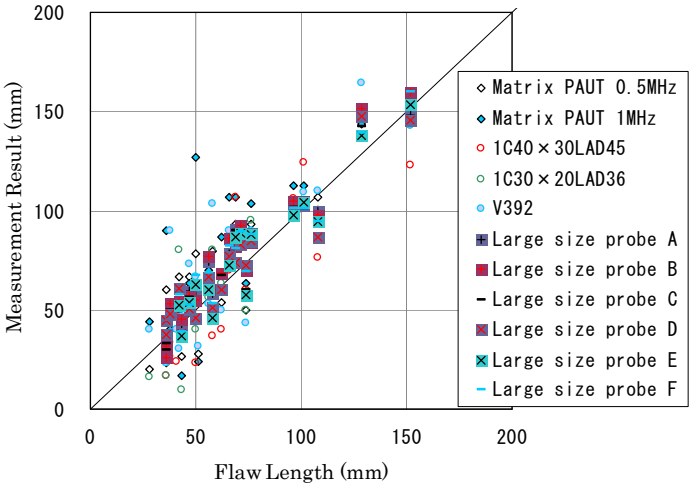

Max. error of overestimation: 76.9mm
Max. error of underestimation: -33.0mm
Ave. error: 5.5mm
Standard deviation of errors: 15.9mm
RMSE: 16.8mm

(1) All measurement methods

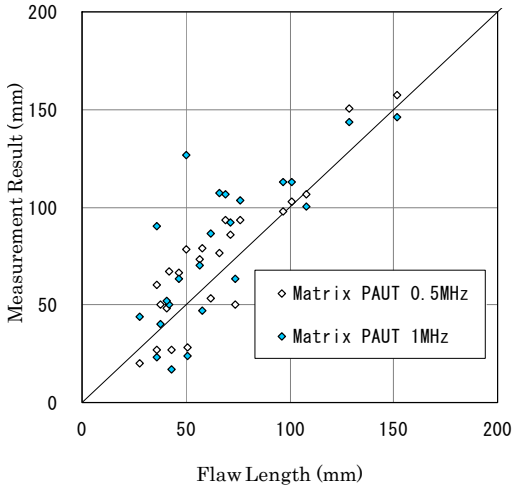

Max. error of overestimation: 76.9mm
Max. error of underestimation: -27.0mm
Ave. error: 9.9mm
Standard deviation of errors: 20.8mm
RMSE: 22.8mm

(2) Matrix PAUT

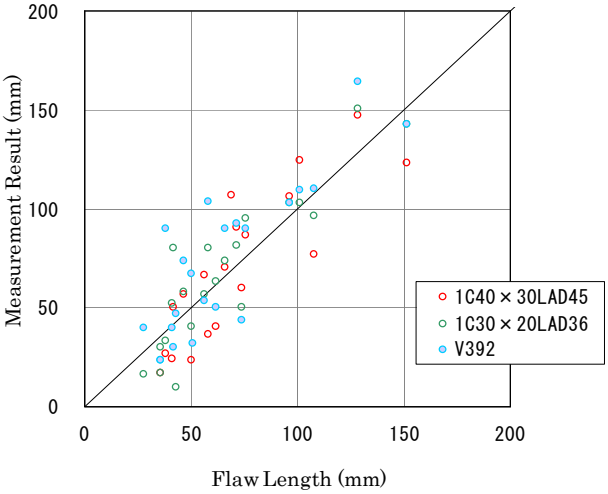

Max. error of overestimation: 52.2mm
Max. error of underestimation: -33.0mm
Ave. error: -2.0mm
Standard deviation of errors: 19.9mm
RMSE: 20.0mm

(3) Conventional UT

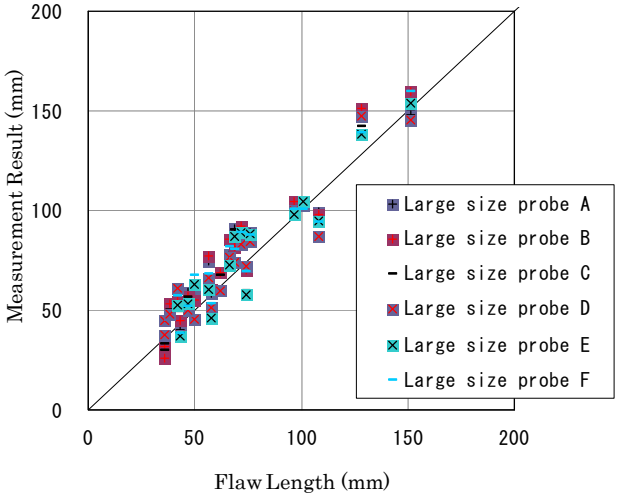

Max. error of overestimation: 23.1mm
Max. error of underestimation: -21.1mm
Ave. error: 5.5mm
Standard deviation of errors: 9.7mm
RMSE: 11.1mm

(4) UT by Large size probe

Fig. 10. Flaw Length sizing accuracy

5. Conclusions

Flaw detection and sizing capabilities for CASS are studied using conventional UT techniques currently applied in in-service inspection program in Japan, PAUT technique and inspection by large size probe. Following conclusions are obtained.

1. Currently available UT techniques are capable to detect the small flaws stable enough under postulated accident loads even after the thermal aging. However, the inspection condition

should be considered when applying the conventional UT technique since a few of techniques was not able to detect 20 mm depth flaw.

2. Regarding flaw sizing capability, inspection using large size probe specially developed for the CASS showed the best results. On the other hand, conventional UT technique had a difficulty to identify the flaw size both in depth and length. PAUT techniques showed improvement of the capability compared to the conventional UT, but still have a room for further improvement to be applied in the field as a flaw sizing technique.

References

[1] Japan Society of Mechanical Engineers, "Code for Nuclear Power Generation Facilities - Rules on Fitness-for-Service for Nuclear Power Plants", JSME S NA 1-2008, October 2008.
[2] Y. Kurozumi, H. Ishida, "Detection Sensitivity and Sizing Ability of Defects in Cast Stainless Steel with Newly Developed Automatic Ultrasonic Inspection System", Journal of the Institute of Nuclear Safety System, 2004, No 7, pp.182-197.
[3] M.T. Anderson, S.E. Cumblidge, S.R. Doctor, "Low Frequency Phased Array Techniques for Crack Detection in Cast Austenitic Piping Welds: A Feasibility Study", Material Evaluations/January 2007, pp.55-61.
[4] M. Anderson, S.Crawford, S. Cumblidge, K. Denslow, A. Diaz, S. Doctor, "Assessment of Crack Detection in Heavy-Walled Cast Stainless Steel Piping Welds Using Advanced Low-Frequency Ultrasonic Methods" U.S. Nuclear Regulatory Commission, NUREG/CR-6933, March 2007.
[5] M.T. Anderson, A.D. Cinson, S.L. Crawford, S.E. Cumblidge, A.A. Diaz, "Research and Evaluation of Advanced Nondestructive Examination (NDE) Methods for Addressing the Challenges of Inspecting Cast Austenitic Stainless Steel (CASS) Piping" Proceedings of the 7th International Conference on NDE in Relation to Structural Integrity for Nuclear and Pressurized Components, May 2009, pp.318-328.
[6] F. Rupin, B. Chassignole, et. al, "Flaw Detection in Cast Stainless Steel Using Advanced Low-Frequency Urtrasonic System and Multi-Scattering Filtering" Proceedings of the 8th International Conference on NDE in Relation to Structural Integrity for Nuclear and Pressurized Components, October 2010, pp.772-781.
[7] Y. Kurozumi, "Development of Ultrasonic Inspection Techniques for Cast Stainless Steel", Journal of the Institute of Nuclear Safety System, 2000, No 7, pp.159-171.
[8] P. Lemaitre, T.D. Koble, "Report on the Evaluation of the Inspection Results of the Cast-to-Cast PISC III Assemblies no. 41, 42 and Weld B of Assembly 43", PISC III Report No. 34, European Commission, 1995.
[9] P. Lemaitre, T.D. Koble, "Report on the Evaluation of the Inspection Results of the Wrought-to-Cast PISC III Assemblies 51 and Weld A of Assembly 43", PISC III Report No. 35, European Commission, 1995.
[10] Japan Nuclear Energy Safety Organization, "Summary Report of the Development on Standards and Guides for Formation of Up-graded Inspection System on NPP regarding Ultrasonic Test and Evaluation for Maintenance Standards", April 2005.
[11] Kazunobu Sakamoto, Takashi Furukawa et. al, "Study on the Ultrasound Propagation in Cast Austenitic Stainless Steel", E-Journal of Advanced Maintenance, EJAM 11-45, to be published.
[12] Japanese Industrial Standards Committee, "Non destructive Testing – Qualification and Certification of Personnel", Japanese Industrial Standard (JIS) Z2305-2001, 2001.
[13] The Japan Society for Non-Destructive Inspection, "Rule for Certification of Nondestructive Testing Personnel", Japanese Nondestructive Inspection Standard (NDIS) 0601, 2000.
[14] S.E. Cumblidge, S.R. Doctor, et. al, "Result of the Program for the Inspection of Nickel Alloy Components", U.S. Nuclear Regulatory Commission, NUREG/CR-7019 (PNNL-18713 Rev.1), August 2010.
[15] Japan Nuclear Energy Safety Organization, "Research Report on the Integrity of Thermally Aged Cast Stainless Steel Piping", JNES-SS report, April 2006.
[16] The Japan Society for Non-Destructive Inspection, "Qualification and Certification of Personnel for Performance Demonstration of Ultrasonic Testing Systems", Japanese Nondestructive Inspection Standard (NDIS) 0603, 2005.
[17] The American Society of Mechanical Engineers, "Rules for Inservice Inspection of Nuclear Power Plant Components", ASME Boilaer and Pressure Vessel Code Section XI, 2010.